

High frequency dielectric properties of CaTiO₃-based microwave ceramics

A Pashkin¹, S Kamba¹, M Berta¹, J Petzelt¹,
G D C Csete de Györgyfalva², H Zheng², H. Bagshaw² and
I M Reaney²

¹ Institute of Physics, Academy of Sciences of the Czech Republic Na Slovance 2,
182 21 Prague 8, Czech Republic

² Department of Engineering Materials, University of Sheffield, Sheffield S1 3JD, UK

Received 15 September 2004, in final form 19 November 2004

Published 18 February 2005

Online at stacks.iop.org/JPhysD/38/741

Abstract

We have investigated the far-IR, submillimetre and microwave (MW) dielectric response of CaTiO₃ (CT)–Sr(Mg_{1/3}Nb_{2/3})O₃ (SMN), CT–Sr(Zn_{1/3}Nb_{2/3})O₃ (SZN), CT–NdAlO₃ (NA) and CT–LaGaO₃ (LG) solid solutions ceramics series. The contribution of extrinsic losses has been analysed by extrapolation of the far-IR and terahertz dielectric data down to the MW range and comparison with directly measured data. This procedure has also been justified by comparing the losses in CT and LG ceramics with the losses in their crystalline forms published in the literature.

The compositional dependences of the permittivity and temperature coefficient on the resonance frequency have been analysed and fitted by appropriate expressions. We have found that in the case of CT–NA and CT–LG ceramics, the best fits can be obtained using a Clausius–Mossotti equation with linearly mixed polarizabilities. On the other hand, for CT–SMN and CT–SZN ceramics the Lichtenecker logarithmic rule and the Hashin–Shtrikman expression have been used. We explain this difference as a consequence of the different character of short-range ordering in the studied ceramic systems.

1. Introduction

Microwave (MW) low-loss ceramics are nowadays widely used as MW dielectric resonators in MW integrated circuits. The basic requirements for MW resonators are small size, high quality factor and good temperature stability. Ceramic technology allows preparation of relatively cheap materials with well defined properties for industrial applications. The permittivity, ϵ' , of such materials should be high enough to reduce the size (proportional to $1/\sqrt{\epsilon'}$) of a resonator and weakly temperature dependent to minimize a temperature coefficient of resonant frequency τ_f . At the same time, the dielectric losses, ϵ'' , should be very low in order to provide a high quality factor, Q , of the resonator ($Q = \epsilon'/\epsilon''$) in the MW range.

Dielectric losses in MW materials consist of *intrinsic losses* which are fundamental losses of multiphonon origin in an ideal crystalline material and *extrinsic losses* caused by lattice defects [1]. Separation of the intrinsic and extrinsic MW losses using standard MW measurements is very difficult. The most promising approach to this problem is to study a higher

frequency dielectric response including the whole terahertz and IR range [2]. This is based on the fact that the fundamental interaction of lattice vibrations with electromagnetic radiation (intrinsic losses) is determined by the parameters of IR-active phonons.

Phonon dispersion can be described by the four-parameter factorized oscillator model [3],

$$\epsilon(\omega) = \epsilon'(\omega) - i\epsilon''(\omega) = \epsilon_\infty \prod_{j=1}^n \frac{\omega_{LO_j}^2 - \omega^2 + i\omega\gamma_{LO_j}}{\omega_{TO_j}^2 - \omega^2 + i\omega\gamma_{TO_j}}, \quad (1)$$

where ω_{TO_j} and ω_{LO_j} are the transverse and longitudinal frequencies of the j th polar phonon mode, respectively, γ_{TO_j} and γ_{LO_j} their respective damping constants and ϵ_∞ the optical permittivity due to the electronic polarization processes. In the low-frequency limit ($\omega \ll \omega_{TO_j}$), equation (1) yields losses which are linearly dependent on frequency, $\epsilon'' \propto \omega$, and a frequency-independent permittivity. However, the oscillator model (1) describes the one-phonon absorption processes, whereas the dielectric losses in the low-frequency limit are determined mostly by two-phonon absorption or higher order

processes. Therefore, formally the oscillator model is not valid in the MW range. A more complicated microscopic theory [1, 4] has to be used to describe the frequency and temperature behaviour of MW losses. However, this theory operates with microscopic parameters which cannot be determined experimentally and therefore it provides only qualitative predictions. In the low-frequency limit, the theory [4] predicts in most crystal symmetries the same linear behaviour, $\epsilon'' \propto \omega$, as follows from the oscillator model. It has been demonstrated that extrapolation of the oscillator model to the MW range gives reasonable results for a great variety of MW ceramics [2, 5–8].

CaTiO₃ (CT) is a good candidate for a MW dielectric since it has a high permittivity, $\epsilon' = 160$, and an acceptable quality factor $Q = 8000$ at 1.5 GHz, but unfortunately it has a large positive temperature coefficient of the resonant frequency ($\tau_f = +850 \text{ ppm K}^{-1}$) [9]. At room temperature it crystallizes in the orthorhombic space group *Pbnm* with four formula units per unit cell. A detailed IR spectroscopic study on CaTiO₃ crystals has been recently reported by Železný *et al* [10]. In order to produce a MW material with τ_f close to zero, one may form a solid solution of CaTiO₃ with a material exhibiting a negative τ_f . We have studied four complex ceramic systems in which CaTiO₃ is mixed in different ratios with perovskites: Sr(Mg_{1/3}Nb_{2/3})O₃ (SMN), Sr(Zn_{1/3}Nb_{2/3})O₃ (SZN), LaGaO₃ (LG) and NdAlO₃ (NA).

Sr(Mg_{1/3}Nb_{2/3})O₃ is a material with a small negative temperature coefficient ($\tau_f = -14 \text{ ppm K}^{-1}$), permittivity $\epsilon = 33$ and $Q = 20\,000$ at 3 GHz [9]. Structural investigation of SMN revealed 1 : 2 stoichiometric B-site cations ordering in a trigonal complex perovskite structure (space group *P $\bar{3}m1$*) [11]; however, recent structural studies revealed an $a^-a^-c^+$ tilt, identical to that of CaTiO₃, and the resulting symmetry is therefore probably monoclinic [12]. In $(1-x)\text{CT}-x\text{SMN}$, a 1 : 2 ordering is maintained only for $x > 0.9$ [12]. Additional evidence for B-site ordering was given by observation of two Raman peaks near 391 and 825 cm^{-1} in CT-SMN, which are not present in pure CaTiO₃ [13]. The first peak is related to the long-range order and vanishes for $x \leq 0.8$. The second peak, at 825 cm^{-1} , is present even for higher concentrations of CaTiO₃ and becomes wider with decreasing x . It was suggested that this may reflect the degree of short-range ordering (nonrandom B-site distribution) in CT-SMN [13]. The temperature coefficient of the resonant frequency, τ_f , passes through zero at $x \simeq 0.8$ with $\epsilon \simeq 45$. However, the reported quality factor, $Q \times f = 11 \text{ THz}$, is rather poor for this composition [12, 13].

LaGaO₃ has attracted much attention as a substrate for epitaxial growth of superconducting YBa₂Cu₃O_{7- δ} films [14]. It possesses very low dielectric losses up to the gigahertz frequency range with a permittivity of $\epsilon \simeq 25$, and therefore it is considered as a promising material for MW applications. LG undergoes a phase transition at 145°C, in which it transforms from a high-temperature orthorhombic *Pnma* phase to a rhombohedral structure with the *R3c* space group [15, 16]. Raman spectroscopy of LG ceramics has been reported in [17, 18]. Fortunately, the dielectric and IR measurements were performed on single crystals, which gives us the possibility of comparing our results on ceramics with them. The IR reflectivity has been measured and fitted by Calvani *et al* [19] and later by Zhang *et al* [20].

Dube *et al* [21] reported low-frequency (100 Hz–1 MHz) and MW dielectric properties of LG single crystals with (001) and (110) orientations. The measured dielectric quality factor for the (001) crystal at room temperature was $Q = 10\,500$ at 7.9 GHz.

NdAlO₃ is a rhombohedral perovskite with $\epsilon \simeq 22$, a good quality factor ($Q \times f \simeq 58\,000 \text{ GHz}$) and a negative temperature coefficient of the resonant frequency ($\tau_f = -33 \text{ ppm K}^{-1}$) [22]. Depending on the chemical composition of the $(1-x)\text{CT}-x\text{NA}$ solid solution, relative permittivities higher than 45 can be obtained with high quality factors ($Q \times f > 40\,000 \text{ GHz}$) and a relatively small temperature coefficient, τ_f . A value of τ_f close to zero has been observed [23] for $x \simeq 0.3$. X-ray analysis shows the existence of at least two distinct regions, depending on the composition. In the range $0 < x < 0.85$ the structure is orthorhombic, like that of pure CaTiO₃ (space group *Pbnm*), and for $x > 0.90$ it is trigonal as in pure NdAlO₃ (space group *R $\bar{3}c$*) [24]. Microstructural characterization of CT-NA ceramics demonstrated that the heating conditions during sintering and subsequent cooling strongly affect the number of structural defects and correspondingly the dielectric losses ($Q \times f$ may vary from 30 000 to 45 000 GHz) [24, 25]. A Raman scattering study of CT-NA revealed short-range ordering of B-site cations which appears as a broad Raman band around 800 cm^{-1} ; this band is absent in both pure CT and NA, and it has the strongest intensity for $x = 0.5$ [13].

In this paper we present the results of combined terahertz and far-IR spectroscopy for CaTiO₃-based ceramics. The dielectric losses extrapolated from the IR fits are compared with the directly measured MW data. In addition, we discuss the compositional dependence of the permittivity, ϵ' , and τ_f for all studied systems. The results for pure CaTiO₃ and LaGaO₃ ceramics are compared with published single crystal data.

2. Experiment

The samples were synthesized by a conventional mixed oxide route using high purity powders of CaCO₃, TiO₂, Nd₂O₃, Al₂O₃, SrCO₃, MgO and Nb₂O₅. The starting reagents were weighed and mixed in the given ratios and milled. The powders were calcined for 4–6 h at temperatures between 1300°C and 1550°C, depending on the composition. The calcined powders were re-milled, pressed into pellets and sintered for 4–6 h at temperatures between 1500 and 1650 K.

All the final ceramics had a density greater than 95% of the theoretical one. The grain size varied from sample to sample, and some typical SEM pictures are shown in figure 1. Most of the ceramics were single phase; only in some CT-LG samples were traces of the second phase observed in the XRD patterns (see figure 2).

MW measurements were performed using an Agilent vector network analyser (8753ES) by the resonant technique. The accuracy of measurement was better than 5%. Details can be found elsewhere [13].

IR reflectivity spectra were obtained using a Fourier transform spectrometer (Bruker IFS 113v) in the frequency range 30–3000 cm^{-1} with 2 cm^{-1} resolution. The samples were prepared in the form of approximately 2 mm thick discs with an optically polished front side.

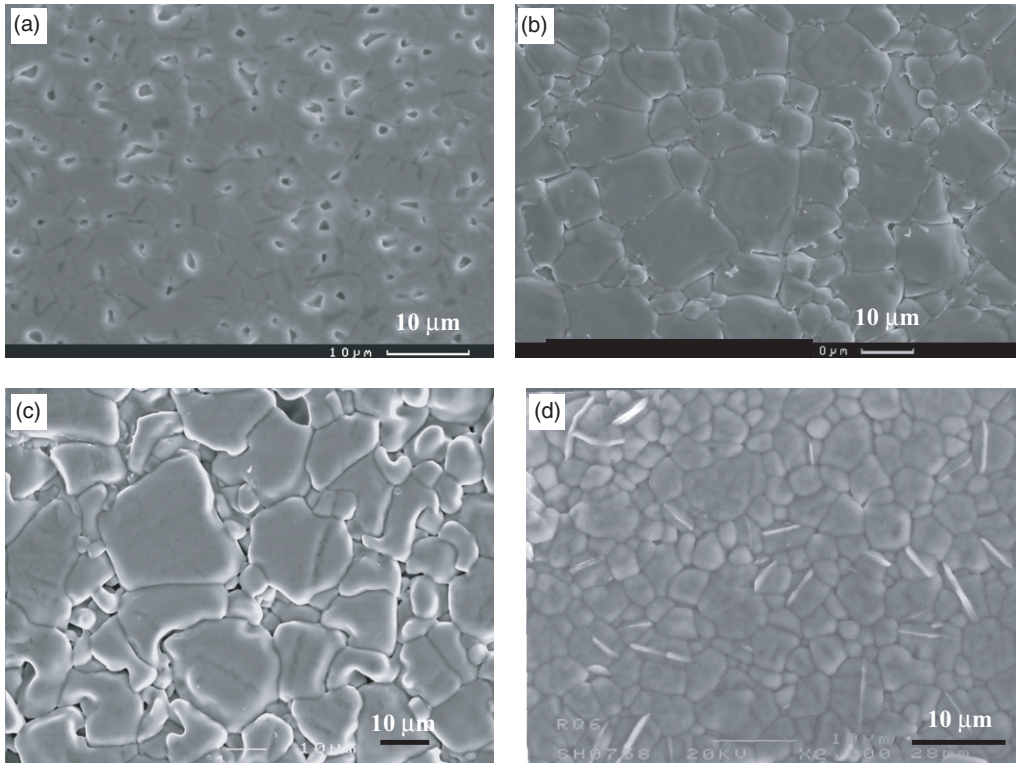


Figure 1. SEM photographs from ceramics: (a) 0.5CT-0.5NA, (b) 0.5CT-0.5LG, (c) 0.5CT-0.5SZN and (d) 0.5CT-0.5SMN.

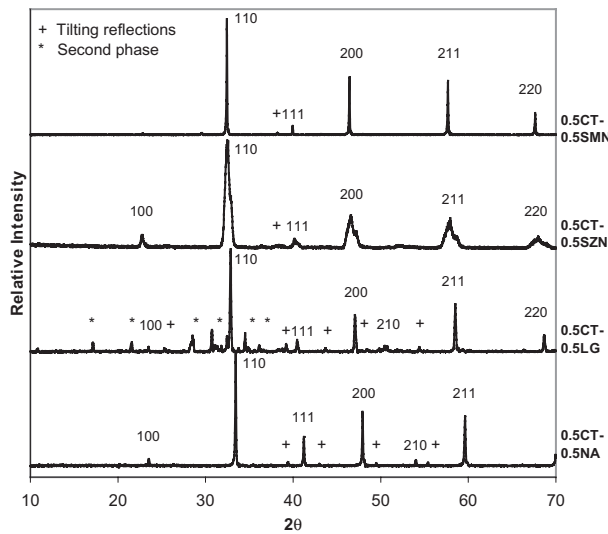


Figure 2. XRD traces from 0.5CT-0.5NA, 0.5CT-0.5LG, 0.5CT-0.5SZN and 0.5CT-0.5SMN ceramics. Traces are indexed according to a pseudocubic unit cell. Peaks marked + result from oxygen octahedral tilting and peaks marked * are associated with the second phase present in 0.5CT-0.5LG.

The measurements of complex terahertz permittivity were carried out using a custom-made time-domain terahertz transmission spectrometer based on an amplified femtosecond laser system. Generation and detection of pulsed terahertz radiation were performed using (110) ZnTe nonlinear optical crystals [26]. The samples for terahertz transmission measurements were prepared in the form of plane-parallel pellets with a diameter of 6 mm and a thickness of

approximately 0.2 mm. The accuracy of terahertz permittivity is limited mainly by errors in the sample thicknesses (plane-parallelity) of about $\pm 1 \mu\text{m}$, so that the terahertz ϵ' is determined with errors of about 1%. The error in the terahertz dielectric loss, ϵ'' , reaches up to 10%, but it can be reduced by an appropriate sample thickness.

The measured far-IR reflectivity spectra have been fitted by the oscillator model (equation (1)) using the expression for the reflectivity under normal incidence:

$$R(\omega) = \left| \frac{\sqrt{\epsilon(\omega)} - 1}{\sqrt{\epsilon(\omega)} + 1} \right|^2. \quad (2)$$

However, it is known that small errors in the reflectivity may lead to appreciable errors in the fitted permittivity and especially in the losses. Therefore the fitting has been carried out taking into account the complex terahertz permittivity which allowed an essential improvement in the quality of the fits. An example, the fitting results for the $(1-x)\text{CT}-x\text{SMN}$ sample with $x = 0.8$, is shown in figure 3. The measured MW permittivity and losses are added for comparison. One can see a good agreement between the measured MW permittivity and that obtained from the fit extrapolation. This is typical for all fitted samples because the permittivity of MW ceramics is fully determined by the contribution of polar phonons and it is not very sensitive to the presence of structural defects. On the other hand, the measured MW losses are usually higher than the intrinsic losses predicted by the fits due to the influence of structural defects which lead to nonvanishing extrinsic losses.

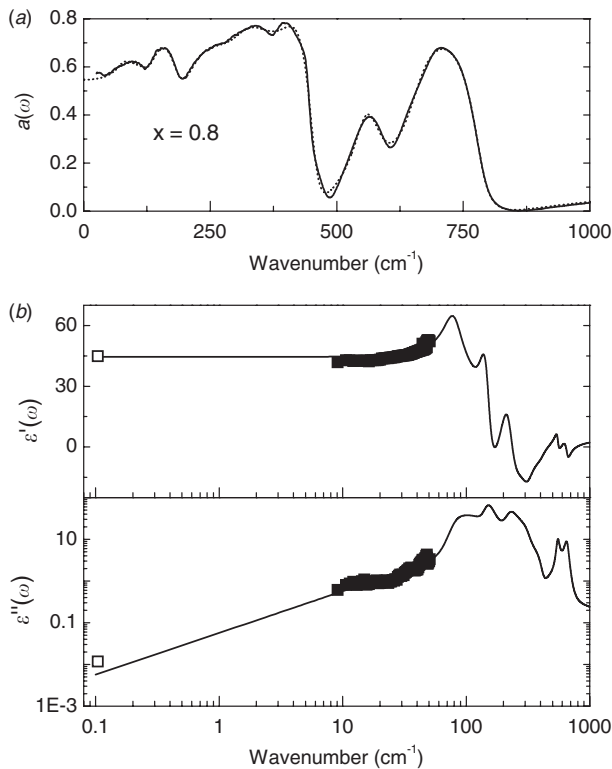


Figure 3. (a) Far-IR reflectivity of $(1-x)\text{CT}-x\text{SMN}$ ($x = 0.8$) ceramics. The solid line is the measured spectrum, the dashed line is the fit. (b) Fitted permittivity and dielectric loss spectra of the same sample. Open symbols correspond to MW data, full symbols correspond to the complex terahertz spectra.

3. Results and discussion

3.1. Comparison with crystalline samples

First, let us compare our results for pure LG and CT ceramics with previous measurements performed on single crystals of LG [20, 21] and CT [10].

Factor group analysis predicts 25 IR-active modes in pure LG at room temperature (space group $Pnma$) [17]. However our fit uses only 11 oscillators. The remaining 14 modes are probably negligibly weak and/or overlap with other modes. We have simulated the dielectric response of the LaGaO_3 crystal using the parameters of the classical oscillator model determined by Zhang *et al* [20]. The total number of oscillators was ten and their parameters are in satisfactory agreement with our fit. The permittivity values obtained are in good agreement: $\epsilon'(0) = 24.3$ from our fit and $\epsilon'(0) = 22.6$ from the fit of Zhang *et al*. The product of the MW quality factor and frequency obtained from the simulation is $Q \times f \simeq 83\,000$ GHz. The same quantity obtained using our fits is slightly higher, $Q \times f \simeq 116\,000$ GHz. Such an agreement between extrapolated MW quality factors indicates that the phonon dynamics in the ceramics is the same as in the single crystal. Taking into account the results of the comparison, we can conclude that the defects in LG ceramics do not affect appreciably the damping or dielectric strength of polar phonon modes in this material.

Let us now compare the directly measured MW quality factors of LaGaO_3 single crystals and ceramics. Dube *et al* [21]

reported $Q = 10\,500$ at 7.9 GHz for an (001)-oriented crystal. However, this values does not refer to the dielectric losses in a particular direction because measurements were carried out using a resonance method and the cylindrical electric field in the cavity does not define the response along a particular crystallographic direction but rather gives an averaged response in the plane normal to the [001] direction. The measured quality factor of our LG ceramics was $Q \simeq 12\,600$ at 4.96 GHz. The corresponding products of the quality factor and measuring frequency are 83 000 GHz for the LG crystal and 62 500 GHz for the LG ceramics. One can also note perfect agreement between the measured MW dielectric losses of the single crystal and intrinsic losses extrapolated from the far-IR range mentioned in the previous paragraph. Thus the dielectric losses of LaGaO_3 single crystals are fully determined by the fundamental phonon absorption processes as could be expected. On the other hand, the dielectric losses of LaGaO_3 ceramics are higher than in single crystal by an amount of extrinsic loss contribution. For the LaGaO_3 ceramic sample investigated (at 4.96 GHz), about 54% of the losses are contributed by the IR-phonon losses and 46% are due to the extrinsic losses.

For the CT single crystal (space group $Pbnm$), factor group analysis predicts 25 IR-active modes though only 14 of them are strong enough to be detected [10]. We have used 13 modes to fit the reflectivity of our CT ceramics. The values of static permittivity of the CT crystal, $\epsilon'(0) = 173$, and ceramics, $\epsilon'(0) = 165$, are in reasonable agreement. However, the MW quality factors estimated from the fits are noticeably different: $Q \times f \simeq 17\,400$ GHz for the CT crystal and $Q \times f \simeq 11\,500$ GHz for CT ceramics. It means that in contrast to LG, the IR dielectric response of CT ceramics might be influenced by some defects which cause an increase in the oscillator damping constants.

To our knowledge, no published measurements exist of CaTiO_3 crystal dielectric losses in the MW range. The well-known publication by Rupprecht and Bell [27] presents the MW permittivities only. The measured MW quality of CT ceramics is 4800 at 2.07 GHz. The corresponding product $Q \times f = 9960$ GHz is somewhat smaller than the losses extrapolated from the IR fit (11 500 GHz). However this difference is not as large as the difference between the extrapolated quality factors of crystalline and ceramic CT. Thus the elevated MW losses in CT ceramics seem to be related to changes in the one-phonon absorption mechanism caused by defects, whereas in LG ceramics the presence of defects affects higher order absorption processes.

3.2. Permittivity dependence on composition

X-ray diffraction analysis has shown that all investigated CaTiO_3 -based complex ceramics systems are predominantly single-phase solid solutions in the whole range of concentrations. It is interesting to see how the dielectric properties (permittivity in particular) depend on the composition of the samples. It was demonstrated that the permittivities in the MW and submillimetre frequency ranges are almost equal in all cases. Therefore we present here only the MW values of permittivity and the temperature coefficient of the resonance frequency at room temperature for all studied samples.

The MW permittivity of the investigated samples is shown in figure 4. One can note that the compositional dependence of the permittivity of the investigated ceramics has a different character. The permittivity of CT decreases rather smoothly with increasing SMN or SZN concentrations. On the other hand, the permittivity of (1 - x)CT-xNA or (1 - x)CT-xLG solid solutions drops to 80 (which is one half of the permittivity of pure CaTiO₃) for a moderate concentration $x = 0.1$. Such a steep compositional dependence of the permittivity has been already reported by Levin *et al* [28] for the Ca(Al_{0.5}Nb_{0.5})O₃-CaTiO₃ (CT-CAN) system. They have demonstrated that this behaviour can be well described by the Clausius-Mossotti equation with linearly mixed polarizabilities of pure components. Thus the resulting permittivity, ϵ , can be found from the following equation [29],

$$\frac{\epsilon - 1}{\epsilon + 2} = (1 - x) \frac{\epsilon_1 - 1}{\epsilon_1 + 2} + x \frac{\epsilon_2 - 1}{\epsilon_2 + 2}, \quad (3)$$

where ϵ_1 and ϵ_2 are the permittivities of the pure components. The least-square fits of the CT-NA and CT-LG systems' permittivity using equation (3) are shown in figure 4. The agreement of the fits with the experimental data is good.

The permittivity of the CT-SMN and CT-SZN systems cannot be described by equation (3). On the other hand, the well-known Maxwell-Garnett and Bruggeman effective medium approximations [30] give overestimated values of the intermediate permittivities. We have found that there are two appropriate formulae in this case. The first is the Lichtenecker empirical logarithmic rule [31],

$$\ln \epsilon = (1 - x) \ln \epsilon_1 + x \ln \epsilon_2. \quad (4)$$

This rule is used sometimes for mixtures of powders or porous systems.

The second appropriate formula is the lower bound of the Hashin-Shtrikman expression for an isotropic composite [32],

$$\epsilon = \epsilon_2 + \frac{1 - x}{1/(\epsilon_2 - \epsilon_1) + x/3\epsilon_1}. \quad (5)$$

This formula describes the precise solution for the permittivity of a mixture of coated spheres. The lower bound corresponds

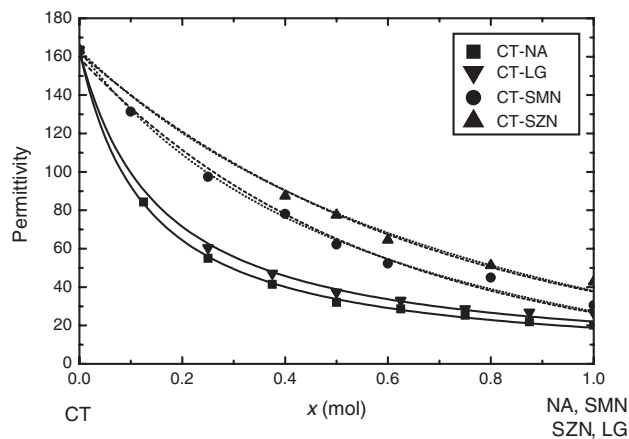


Figure 4. MW permittivity of CaTiO₃-based solid solutions. Solid, dashed and dotted lines are fits by equation (3), equation (4) and equation (5), respectively.

to the case where the component with the higher permittivity (ϵ_1) is covered by the low-permittivity component (ϵ_2) and therefore is not percolated.

The fits using equations (4) and (5) are shown in figure 4. The correspondence between the fits and the measured MW data is reasonable for both cases. However, the Lichtenecker rule is an empirical expression and the Hashin-Shtrikman expression corresponds to an idealized mixture geometry. Therefore it is not worth speculating which of these equations is more relevant to the real situation in CT-SMN and CT-SZN systems.

The different character of permittivity behaviour in CaTiO₃-based systems may be related to the structural properties of the mixed components and solid solutions. The short-range order inherent to Sr(Mg_{1/3}Nb_{2/3})O₃ persists in CT-SMN system for all intermediate concentrations as has been revealed from Raman spectra [13]. Similar behaviour is expected for the CT-SZN system. In contrast, the Raman band corresponding to short-range order in the CT-CAN system vanishes when CaTiO₃ constitutes more than half of the composition [28] ($x > 0.5$).

On the other hand, the short-range order in the CT-NA system corresponds to ordering of the CaTiO₃ and NdAlO₃ unit cells. In this respect, the components of the CT-NA (and probably CT-LG) solid solutions are perfectly mixed. Thus, the permittivity of the CT-NA and CT-LG systems as well as the permittivity of the CT-CAN system is described by the Clausius-Mossotti equation with effectively mixed polarizabilities. SMN and SZN in CaTiO₃-based solutions may tend to preserve their ordered structure and do not perfectly mix with CaTiO₃ at the microscopic level. Therefore, the permittivity behaviour of the CT-SMN and CT-SZN systems deviates from equation (3) and is better described by the Lichtenecker or Hashin-Shtrikman expressions for the mixture of macroscopically large particles.

Figure 5 shows the compositional dependence of τ_f for the ceramics systems investigated. Compositions that correspond to the temperature stable permittivity ($\tau_f \simeq 0$) are $x \simeq 0.85$ for CT-SMN and CT-SZN systems; $x \simeq 0.36$ for CT-LG; and $x \simeq 0.43$ for CT-NA. The concentrations found for CT-SMN and CT-NA are in reasonable agreement with the values of $x = 0.8$ and $x = 0.375$ recently reported by some of the

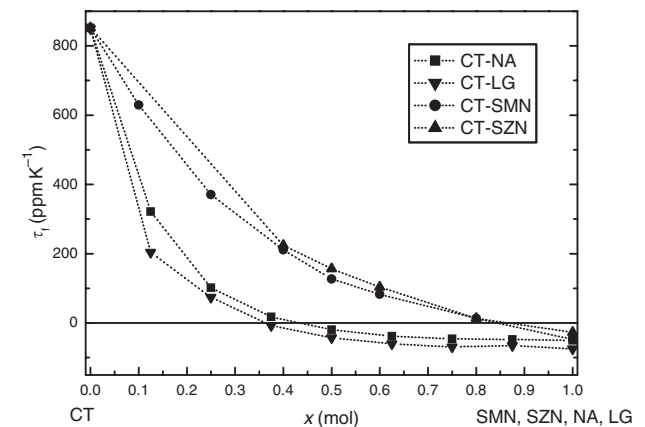


Figure 5. τ_f as a function of concentration, x , for CaTiO₃-based solid solutions.

present authors [12, 13]. However, other authors obtained $\tau_f \approx 0$ in CT-NA for lower $x = 0.3$ [23–25].

We have tried to describe the compositional dependence of τ_f using the known permittivities and temperature coefficients of the pure compounds. Following Levin *et al* [28], we assumed the same thermal expansion coefficient $\alpha = 10 \text{ ppm K}^{-1}$ for all compositions. The calculated values of τ_f are overestimated compared with the measured values in all cases. Nevertheless, the qualitative behaviour is reproduced rather well.

3.3. Dielectric losses

3.3.1. CT-SMN ceramics. In the case of ordered $A(B'_{1/3}B''_{2/3})O_3$ compounds (SMN is a particular case), factor group analysis in the paraelectric phase ($P\bar{3}m1$, $Z = 3$) yields 16 IR-active modes [33]. Pure CaTiO_3 displays 25 IR-active modes (only 14 of them are strong enough to be detected [10]). We have used 16 four-parameter oscillators for the fitting of pure SMN, 9 for $0.4 \leq x \leq 0.8$, where long-range ordering of B-sites does not exist, and 11–13 for $x \leq 0.25$. The measured reflectivity of pure SMN ceramics agrees with the data published by Fukuda *et al* [34]. However they used 20 oscillators for the fitting of reflectivity, which is probably redundant for SMN, in our opinion.

The products of the quality factor and frequency, $Q \times f$, measured in the MW range and those obtained from the fits are plotted as functions of the CT-SMN composition in figure 6(a). The quality factors tend to decrease when the concentration of

SMN is decreasing; however, this dependence is steeper in the case of losses obtained from IR data fits. Thus for $x \leq 0.1$ the dielectric losses are fully determined by the fundamental intrinsic losses and for $x = 0.8$ the extrapolated quality factor is half as small as the measured one. Taking into account the comparison in figure 6(a), we can conclude that the poor quality factor of CT-SMN ceramics with $\tau_f \approx 0$ ($x \approx 0.8$) is mostly a consequence of extrinsic losses which may be eliminated by reducing the defect density in the ceramics. The nature of the defects is not clear from our experiment, but the low-temperature MW and terahertz measurements can, in principle, give more information about the kind of defect in the ceramics [1]. On the other hand, the MW dielectric losses are rather close to the fitted intrinsic losses for 10 and 25 mol% SMN concentration. It indicates a high quality of CT-SMN ceramics with a moderate concentration of SMN.

3.3.2. CT-SZN ceramics. Ordered $\text{Sr}(\text{Zn}_{1/3}\text{Nb}_{2/3})\text{O}_3$ has the same structure as SMN, a slightly higher permittivity $\epsilon \approx 43$ and a quality factor ($Q = 3850$ at 3 GHz) which is appreciably lower than that of SMN. The temperature coefficient of the resonance frequency in SZN is $\tau_f = -26.8 \text{ ppm K}^{-1}$. $(1-x)\text{CT}-x\text{SZN}$ solid solutions have not been investigated in the MW and far-IR ranges until recently. Initial x-ray diffraction studies revealed a perovskite structure in the full range of concentrations. Therefore, despite the rather high dielectric losses in the CT-SZN system, its investigation is interesting from the point of view of comparison with CT-SMN. The important point is that a temperature-stable MW ceramic with high permittivity can be obtained.

The number of IR modes used for the fitting of FTIR reflectivity and TDTTS complex permittivity data was varied from 8 (for $x = 0.6$) to 16 (for $x = 1$). The measured reflectivity and the fit parameters of pure SZN agree with previously published data [34]. The comparison between the measured quality factors and those predicted by IR fits is shown in figure 6(b). For $0 < x < 0.4$ the losses are so high that the resonance in the MW cavity was suppressed. The measured $Q \times f$ values are lower than those obtained from the fits. However this difference is not so pronounced as in the case of CT-SMN system. The MW losses become appreciably higher than the intrinsic losses only for $x \leq 0.4$. Thus we can conclude that the low quality factors of CT-SZN ceramics (for $x > 0.4$) are mostly related to the fundamental (intrinsic) loss mechanisms due to multiphonon absorption processes. In contrast to the case with CT-SMN ceramics, there seems to be no technological way of obtaining an appreciably higher quality of the CT-SZN ceramics investigated.

3.3.3. CT-LG ceramics. The number of oscillators required to obtain good fits varies from 9 to 12 depending on the sample composition. Factor group analysis predicts 25 IR-active modes in LaGaO_3 [17] and the same number of modes in pure CaTiO_3 [10] though its space group, $Pbnm$, is different from the $Pnma$ group of LaGaO_3 . The rest of the predicted modes which have not been observed by experiment are probably very weak and their influence on the dielectric permittivity and losses is negligible.

A comparison between the measured quality factors $Q \times f$ of CT-LG ceramics and those predicted by IR fits is shown

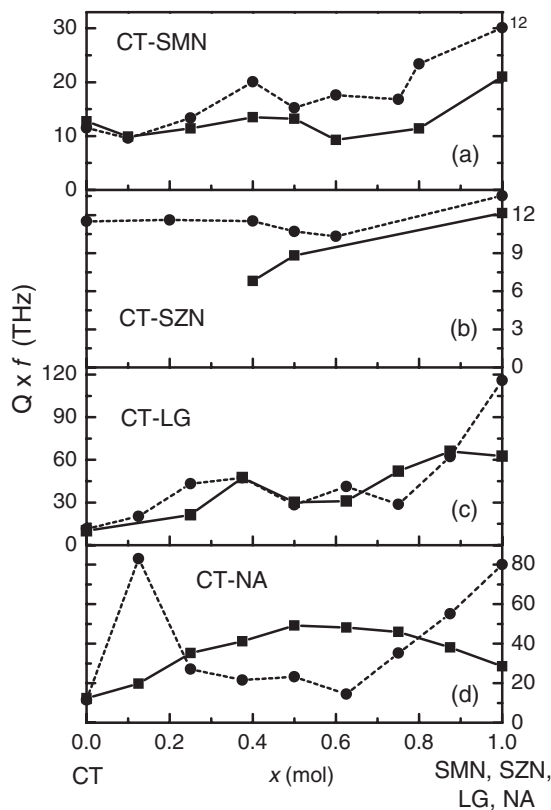


Figure 6. $Q \times f$ values of CaTiO_3 -based ceramics extrapolated from the fits of IR data (●) and directly measured at MW frequencies (■).

in figure 6(c). The MW dielectric losses are higher than the extrapolated intrinsic losses for $x = 1$ and $x = 0.25$, indicating the presence of additional extrinsic losses for these compositions. Other CT-LG ceramics show only slight deviations from the IR fits within the limits of fitting precision.

The MW losses of CT-LG ceramics seem to be mostly determined by intrinsic losses except pure LaGaO₃ and $x = 0.25$, where a pronounced contribution of extrinsic losses is seen.

3.3.4. CT-NA ceramics. The spectra of the dielectric losses of CT-NA ceramics are shown in figure 7. The number of oscillators required to obtain good fits varies from 11 to 13, depending on the sample composition. Factor group analysis predicts eight IR-active modes for pure NA [17]. The agreement between the number of predicted and observed IR-active modes is thus considered to be reasonable with the exception of pure NA, where the activation of four additional weak modes can be due to a partial relaxation of the selection rules related to the existence of the symmetry-breaking defects in the ceramic sample.

It is seen from figures 7 and 6(d) that the linear extrapolation of the dielectric loss from the terahertz to the MW range from the oscillator model gives overestimated losses for intermediate concentrations of CT ($0.25 < x \leq 0.75$). Moreover, the terahertz loss data are also slightly below the values predicted by the fits for this range of concentrations, though the reflectivity curves are perfectly described by the fits. Actually, the oscillator model is exactly valid only close to the phonon frequencies and it can fail at $\omega \ll \omega_{TO}$. Nonetheless our experience obtained from many ceramics shows that the extrapolation of the oscillator model from the terahertz range to the MW range describes well the intrinsic losses in many systems. The CT-NA system seems to be an exception to this rule, in contrast with other CT-based MW ceramics investigated. Nevertheless, one can see that the measured submillimetre losses can be linearly extrapolated to the MW loss values (dotted lines in figure 7). This fact agrees with the predictions of the microscopic theory of intrinsic losses [4] which should correctly describe the losses in the CT-NA system.

Since the oscillator model fails in the case of CT-NA, the only conclusion we can arrive at from comparison of the submillimetre and MW losses is the absence of appreciable extrinsic losses for $0.125 \leq x \leq 0.75$. The pure NA sample and CT-NA with $x = 0.875$ have extrinsic losses which are due to a lower sample quality. Thus CT-NA ceramics with compositions close to the point of temperature stability ($x \approx 0.43$ according to our MW data) can be considered as promising materials for MW applications.

4. Conclusion

Far-IR, submillimetre and MW dielectric responses of CT-SMN, CT-SZN, CT-NA and CT-LG solid solution ceramic series were studied. The intrinsic losses in LaGaO₃ ceramics are almost identical to those of a single crystal [20, 21]. In CaTiO₃ ceramics the intrinsic losses are higher than in the single crystal due to enhanced damping of IR phonons probably caused by structural defects. Thus the

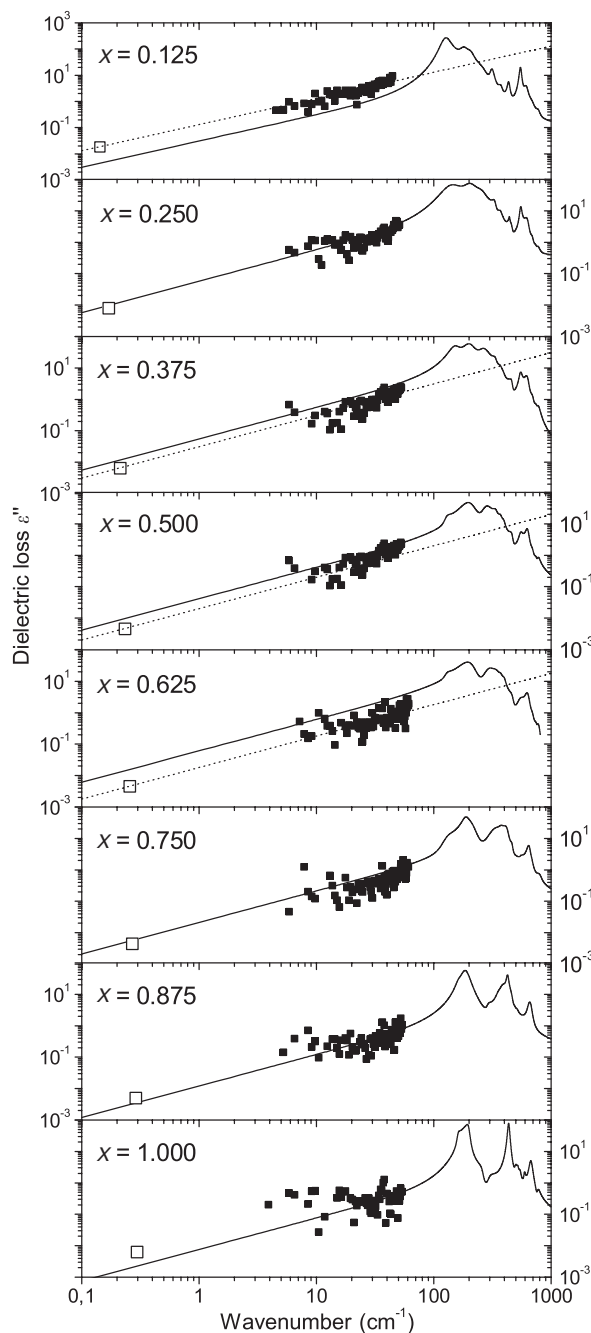


Figure 7. The dielectric loss spectra of $(1-x)\text{CT}-x\text{NA}$ ceramics. The solid lines correspond to the reflectivity fits. The full symbols are the measured terahertz data and the open symbols are the MW losses. The dotted lines are linear fits of the measured terahertz and MW losses.

dielectric losses determined by IR phonons in CaTiO₃ ceramics are not intrinsic in the sense that they would describe only fundamental losses of a perfect crystal.

The compositional dependence of the permittivity of CT-NA and CT-LG ceramics can be described by the Clausius–Mossotti equation with linearly mixed polarizabilities. On the other hand, this dependence for CT-SMN and CT-SZN, where CaTiO₃ is mixed with complex compounds, can be fitted by the Lichtenecker logarithmic formula or the Hashin–Shtrikman model. This difference is

a consequence of the different character of short-range ordering in the ceramic systems studied.

The comparison of extrapolated far-IR and MW losses led to the following conclusions:

The poor MW quality factor of $(1-x)\text{CT}-x\text{SMN}$ ceramics with $\tau_f \approx 0$ ($x \approx 0.8$) is mostly a consequence of some extrinsic losses because the intrinsic quality obtained from the extrapolation of terahertz data is twice as high. The extrinsic losses can be reduced by optimizing the ceramic processing. For CaTiO_3 ceramics moderately doped with SMN, the MW dielectric losses, are rather close to the fitted intrinsic losses, which indicates their high quality.

The low quality factors of CT-SZN ceramics are mostly related to fundamental loss mechanisms. In contrast to CT-SMN ceramics, there is probably no technological way of obtaining appreciably higher quality in them.

The MW losses of CT-LG ceramics are mostly determined by the intrinsic losses except pure LaGaO_3 and compositions with $x \leq 0.25$, where a pronounced contribution of the extrinsic losses is seen.

Extrapolation of the oscillator model fails in some cases for $(1-x)\text{CT}-x\text{NA}$. Nevertheless, CT-NA ceramics with compositions close to the point of temperature stability ($x \approx 0.44$) have such a high quality, Q , that they have already been used in MW applications.

Acknowledgments

The work was supported by the Czech Academy of Sciences (project nos. A1010213, AVOZ01-010-914 and K1010104) and the Grant Agency of the Czech Republic (project no. 202/04/0993). The financial support of the Ministry of Education of the Czech Republic (project no. LN00A032) is also acknowledged.

References

- [1] Petzelt J and Setter N 1993 *Ferroelectrics* **150** 89
- [2] Petzelt J, Kamba S, Kozlov G V and Volkov A A 1996 *Ferroelectrics* **176** 145
- [3] Gervais F 1983 *Infrared and Millimetre Waves* vol 8 (New York: Academic)
- [4] Gurevich V L and Tagantsev A K 1991 *Adv. Phys.* **40** 719
- [5] Petzelt J, Zurmühlen R, Bell A, Kamba S, Kozlov G V, Volkov A A and Setter N 1992 *Ferroelectrics* **133** 205
- [6] Zurmühlen R, Petzelt J, Kamba S, Kozlov G, Volkov A, Gorshunov B, Dube D, Tagantsev A and Setter N 1995 *J. Appl. Phys.* **77** 5351
- [7] Kamba S, Petzelt J, Buixaderas E, Haubrich D, Vaněk P, Kužel P, Jawahar I N, Sebastian M T and Mohanan P 2001 *J. Appl. Phys.* **89** 3900
- [8] Petzelt J and Kamba S 2003 *Mater. Chem. Phys.* **79** 175
- [9] Nomura S 1983 *Ferroelectrics* **49** 61
- [10] Železný V, Cockayne E, Petzelt J, Limonov M F, Usvyat D E, Lemanov V V and Volkov A A 2002 *Phys. Rev. B* **66** 224303
- [11] Zheng H, Csete de Györgyfalva G D C, Quimby R, Bagshaw H, Ubic R, Reaney I M and Yarwood J 2003 *J. Eur. Ceram. Soc.* **23** 2653
- [12] Bagshaw H, Iddles D, Quimby R and Reaney I M 2003 *J. Eur. Ceram. Soc.* **23** 2435
- [13] Zheng H, Csete de Györgyfalva G D C, Quimby R, Bagshaw H, Ubic R, Reaney I M and Yarwood J 2003 *J. Appl. Phys.* **94** 2948
- [14] Sandstrom R L, Giess E A, Gallagher W J, Segmüller A, Cooper E I, Chisholm M F, Gupta A, Shinde S and Laibowitz R B 1988 *Appl. Phys. Lett.* **53** 1874
- [15] Kobayashi J, Tazoh Y, Sasaura M and Miyazawa S 1991 *J. Mater. Res.* **6** 97
- [16] Howard C J and Kennedy B J 1999 *J. Phys.: Condens. Matter* **11** 3229
- [17] Tompsett G A, Sammes N M and Phillips R J 1999 *J. Raman Spectrosc.* **30** 497
- [18] Inagaki T, Miura K, Yoshida H, Fujita J and Nishimura M 1999 *Solid State Ion.* **118** 265
- [19] Calvani P, Capizzi M, Donato F, Dore P, Lupi S, Maselli P and Varsamis C P 1991 *Physica C* **181** 289
- [20] Zhang Z M, Choi B I, Flik M I and Anderson A C 1994 *J. Opt. Soc. Am. B* **11** 2252
- [21] Dube D C, Scheel H J, Reaney I, Daghli M and Setter N 1994 *J. Appl. Phys.* **75** 4126
- [22] Cho S Y, Kim I T and Hong K S 1999 *J. Mater. Res.* **14** 114
- [23] Jančar B, Suvorov D and Valant M 2001 *J. Mater. Sci. Lett.* **20** 71
- [24] Jančar B, Suvorov D, Valant M and Drazic G 2003 *J. Eur. Ceram. Soc.* **23** 1391
- [25] Suvorov D, Valant M, Jančar B and Škapin D 2001 *Acta Chim. Slov.* **48** 87
- [26] Grüner G (ed) 1998 *Millimeter and Submillimeter Wave Spectroscopy of Solids* (Berlin: Springer)
- [27] Rupprecht G and Bell R O 1964 *Phys. Rev.* **135** A748
- [28] Levin I, Chan J Y, Maslar J E, Vanderah T A and Bell S M 2001 *J. Appl. Phys.* **90** 904
- [29] Böttcher C J F 1973 *Theory of Electric Polarization* 2nd edn (Amsterdam: Elsevier)
- [30] Carr G L, Perkowitz S and Tanner D B 1985 *Infrared and Millimeter Waves* (New York: Academic)
- [31] Lichtenecker K 1926 *Phys. Z.* **27** 115
- [32] Bergman D J and Stroud D 1992 *Physical Properties of Macroscopically Inhomogeneous Media* vol 46 *Solid State Phys.* (Boston: Academic)
- [33] Tamura H, Sagala D A and Wakino K 1986 *Japan. J. Appl. Phys.* **25** 787
- [34] Fukuda K, Kitoh R and Awai I 1994 *J. Am. Ceram. Soc.* **77** 149